

ACOUSTIC IMAGING IN SEMI-GEODESIC COORDINATES, NUMERICAL EXPERIMENT

Nosikova V.V.^{}, Pestov L.N.^{}¹

Abstract The problem of imaging of discontinuities of the velocity function by the data of the inverse problem for the wave equation is considered. A method of imaging in semi-geodesic coordinates based on the Blagoveshchenskii formula is used. The results of numerical modeling are presented.

Key words: Acoustic imaging, Blagoveshchenskii's formula, Boundary Control method, triangular factorization.

AMS Mathematics Subject Classification: 35R30.

DOI: 10.32523/2306-6172-2025-13-3-68-74.

1 Introduction

Let u be a solution to the following (forward) problem for the wave equation

$$\frac{1}{c^2(x, y)} u_{tt} = u_{xx} + u_{yy}, \quad \infty < x < \infty \quad y > 0, \quad t > 0, \quad (1)$$

$$u|_{t=0} = 0, \quad u_t|_{t=0} = 0, \quad (2)$$

$$u_y|_{y=0} = f\delta_{x_\alpha}, \quad (3)$$

where $f \in C_0^\infty(0, t_0)$ is a short impulse, $\delta_{x_\alpha}(x) = \delta(x - x_\alpha)$ is the Dirac function supported at point $x_\alpha \in \Gamma_0 \subset \Gamma$, where Γ is the x -axis, velocity c is assumed to be piecewise smooth. Inverse data

$$u^0(x, t; x_\alpha) = u(x, 0, t; x_\alpha), \quad x \in \Gamma_0$$

are given at the same segment where sources located. We consider the problem of imaging discontinuities of the velocity by the inverse data.

One of the main procedures in seismic data processing is migration (reverse-time migration, Kirchhoff migration [1], etc.) which gives an image of the acoustic (seismic) medium. In this case, as a rule, the velocity function is considered to be given. An error in velocity setting can lead to large distortions in the image. In the present work, we assume that velocity is unknown and use the approach for acoustic imaging in semi-geodesic coordinates which was proposed in [2]. This approach is based on the Blagoveshchenskii formula of the scalar product of waves, which is one of the basic tools of the Boundary Control method. Being written in semi-geodesic coordinates, this formula leads to the possibility of determining waves propagating in an unknown medium. This possibility is based on triangular decomposition of the matrix C of the scalar products. Possessing such waves, one can construct an image of the acoustic medium in semi-geodesic coordinates. Another ingredient of our approach is an imaging condition associated with discontinuities of the velocity. The term imaging condition comes from seismic processing, where it is used in migration, and means a formula for imaging.

Triangular factorization of the connecting operator C (in our case matrix) is the main procedure of the Boundary Control method for visualizing waves. First, it was mentioned in [3], (see also [4], [5], [6]). There are many works that contain results on numerical modeling using the Boundary Control method. They are mainly related to solving the inverse problem (velocity restoration) based on solving the boundary control problem ([7],[8],[9],[10],[11]). We do not solve the inverse problem, but visualize an acoustic media based on direct triangular factorization and some formula for imaging.

This article is a continuation of the works [2],[12].

¹Corresponding Author.

2 Imaging condition

We denote by $B(x_\alpha, t) = \{(x, y) \in \mathbb{R}_+^2 \mid \text{dist}((x, y), (x_\alpha, 0)) < t\}$ the riemannian hemi-ball of radius t and centered at $(x_\alpha, 0)$ (the distance between the points (x, y) and $(x_\alpha, 0)$ is understood in the sense of riemannian metric δ^{ij}/c^2). Notice that wave $u(x, y, t; x_\alpha)$ is supported in $B(x_\alpha, t)$. For simplicity, we assume that the velocity is a constant near the boundary. In the following lemma t_0 is the length of the impulse f .

Lemma. *Let $c|_{B(x_\alpha, t_0)} = c_0 = \text{const}$, $\forall x_\alpha \in \Gamma_0$. Then the following equality $\text{sing supp } u(\cdot, \cdot, t, x_\alpha) = \text{sing supp } c \cap \overline{B}(x_\alpha, t)$ holds for $t \geq t_0$.*

Proof. The fundamental solution to the two-dimensional wave equation is

$$K(x, y, t) = \frac{1}{2\pi c_0 \sqrt{c_0^2 t^2 - x^2 - y^2}} H(c_0 t - \sqrt{x^2 + y^2}),$$

where H is the Heaviside function. It coincides (up to factor $1/2$) with the Green function of the Neumann problem. Then for source $f\delta_{x_\alpha}$ we have solution to the problem with constant velocity

$$u_0(x, y, t; x_\alpha) = (f * K)(x - x_\alpha, y, t) = \frac{1}{4\pi c_0} \int_{\sqrt{(x-x_\alpha)^2 + y^2}/c_0}^t \frac{f(t-s)ds}{\sqrt{c_0^2 s^2 - (x-x_\alpha)^2 - y^2}}.$$

From $f \in C_0^\infty(0, t_0)$ it follows that $u_0, \partial_t u_0 \in C^\infty(B(x_\alpha, t_0))$ (it may be shown by integrating by parts). Clearly $u = u_0$ for $t \leq t_0$. Then we have for $t > t_0$

$$u_{xx} + u_{yy} = \frac{1}{c^2(x, y)} u_{tt}, \quad (4)$$

$$u|_{t=t_0} = u_0|_{t=t_0}, \quad u_t|_{t=t_0} = u_{0t}|_{t=t_0}, \quad (5)$$

$$u_y|_{y=0} = 0. \quad (6)$$

Problem (4)-(6) has unique solution in $H^1(B(x_\alpha, T) \times [t_0, T])$ for $T > t_0$ (this is easy to show, following the method of a priori estimates in [13]). Moreover, due to the smoothness of f the solution is smooth in time, $u \in C^\infty([t_0, T]; H^1(B(x_\alpha, T)))$, and then u is smooth everywhere the velocity is smooth. Indeed, let c be smooth in some neighborhood $U_{x,y}$ of point (x, y) . Then from (4) we have $u_{xx} + u_{yy} \in C^\infty([t_0, T]; H^1(U_{x,y}))$. This implies $u \in C^\infty([t_0, T]; H^3(U_{x,y}))$. It follows from the well-known property of elliptic operators about smoothness [14] (in our case the smoothness of u is greater than the smoothness of $u_{xx} + u_{yy}$ by two). Proceeding we have $u \in C^\infty([t_0, T] \times U_{x,y})$. And vice versa, if $u \in C^\infty([t_0, t] \times U_{x,y})$, then from (4) it follows that c is smooth in $U_{x,y}$. \square

Thus, the waves (its derivatives) from all sources have discontinuities at the same set $\text{supp } c$. Based on this, we propose the following formula for imaging (imaging condition) of velocity discontinuities:

$$F(x, y) := \sum_\alpha \int_0^T u_t^2(x, y, t; x_\alpha) dt, \quad (x, y) \in \Omega^T. \quad (7)$$

Strictly speaking, formula (7) is of empiric character. Below (section Forward problem) we show an example of how it works for single source and for all sources.

3 Matrix C

Our approach to imaging is based on the Blagovestchenskii formula for scalar product of waves [15]. We derive shortly this formula in a form, convenient for us. For any solutions u, v to the wave equation the identity

$$\frac{1}{c^2}(u_t v_t + (\nabla u, \nabla v)) = \text{div}(u_t \nabla v + v_t \nabla u)$$

holds. Let $t_\alpha, t_\beta \in [0, T]$, $t_\alpha \leq t_\beta$, $x_\alpha, x_\beta \in \Gamma_0$,

$$v(x, y, t) = \frac{1}{2}[u(x, y, t - t_\alpha + t_\beta; x_\beta) - u(x, y, t_\alpha - t + t_\beta; x_\beta)]$$

and u is $u(x, y, t; x_\alpha)$. Integrating (2) over $\mathbb{R}_+^2 \times [0, t_\alpha]$ and due to $v(x, y, t_\alpha) = 0, v_t(x, y, t_\alpha) = u_t(x, y, t_\beta; x_\beta)$ we get

$$\begin{aligned}
C_{\alpha\beta} &:= \int_{\Omega^T} u_t(x, y, t_\alpha; x_\alpha) u_t(x, y, t_\beta; x_\beta) \frac{dx dy}{c^2(x, y)} = \\
&= \frac{1}{2} \int_0^{t_\alpha} u_t^0(x_\beta, t_\alpha - t; x_\alpha) [f(t_\beta - t) - f(t_\beta + t)] dt \\
&+ \frac{1}{2} \int_0^{t_\alpha} f(t_\alpha - t) [u_t^0(x_\alpha; t_\beta - t, x_\beta) + u_t^0(x_\alpha, t_\beta + t; x_\beta)] dt.
\end{aligned} \tag{8}$$

Here Ω^T is the domain filled up with waves up to the moment T , $\Omega^T = \bigcup_{x_\alpha \in \Gamma_0} B(x_\alpha, T)$. Notice that right hand side of (8) is symmetric w.r.t. α, β . We will call numbers α, β controls. Each control α determines source x_α and radius t_α of hemi-ball $B(x_\alpha, t_\alpha)$.

Introduce semi-geodesic coordinates (x', τ) of point (x, y) (Fig. 1)

$$(x, y) = \gamma(x', \tau), \quad x' \in \Gamma, \quad \tau \in [0, T],$$

where $\gamma(x', \tau)$ is the segment of the geodesic starting from point $x' \in \Gamma$ orthogonally to the boundary of the length $\tau = \text{dist}(x, y; x', 0)$. We assume that the map $\gamma : (x', \tau) \mapsto \gamma(x', \tau)$ is a diffeomorphism $\Gamma \times [0, T]$ on its range. This is true for small enough T . In the semi-geodesic coordinates we have

$$C_{\alpha\beta} = \int_{\gamma^{-1}(\Omega^T)} \frac{J(x', \tau)}{c^2(\gamma(x', \tau))} u_t(\gamma(x', \tau), t_\alpha; x_\alpha) u_t(\gamma(x', \tau), t_\beta; x_\beta) dx' d\tau,$$

where $J(x', \tau)$ is the Jacobian of the map γ .

We rewrite this in the form

$$C_{\alpha\beta} = \int_{\gamma^{-1}(\Omega^T)} v(x', \tau, t_\alpha, x_\alpha) v(x', \tau, t_\beta, x_\beta) dx' d\tau,$$

where

$$v(x', \tau, t_\alpha, x_\alpha) = \frac{\sqrt{J(x', \tau)}}{c(\gamma(x', \tau))} u_t(\gamma(x', \tau), t_\alpha; x_\alpha).$$

If $\Gamma_0 = \Gamma$, the domain $\gamma^{-1}(\Omega^T)$ is known, $\gamma^{-1}(\Omega^T) = \Gamma \times [0, T]$. In our case $\Gamma_0 \neq \Gamma$, and domain $\gamma^{-1}(\Omega^T)$ is unknown. We replace domain $\gamma^{-1}(\Omega^T)$ with $\Gamma_0 \times [0, T] = \Sigma$. By doing so, we introduce an error in the integral. So in what follows

$$C_{\alpha\beta} = \int_{\Sigma} v(x', \tau, t_\alpha, x_\alpha) v(x', \tau, t_\beta, x_\beta) dx' d\tau. \tag{9}$$

We call domain Σ screen following M.I. Belishev and $v(\cdot, \cdot, t_\alpha, x_\alpha)$ wave on the screen, generated by control α . It is on the screen that we will obtain the image according to the following formula

$$F'(x', \tau) = \sum_{\alpha} \int_0^T v^2(x', \tau, t, x_\alpha) dt, \quad (x', \tau) \in \Sigma. \tag{10}$$

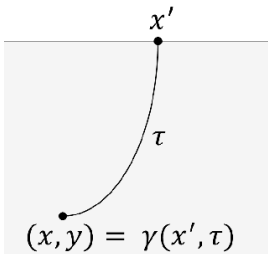


Figure 1: Semi-geodesic coordinates

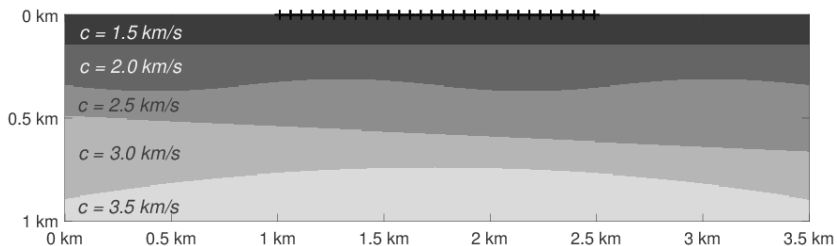


Figure 2: Model

4 Forward problem

In our numerical experiment, we used the two-dimensional layered model (Fig. 2).

To solve the forward problem we used finite difference time domain method (FDTD) for the first-order acoustic system for $p = u_t$ and $V = \nabla u$:

$$\frac{1}{c^2} p_t = \operatorname{div} V, \quad V_t = \nabla p.$$

As the impulse $f(t)$ we used the (truncated) Ricker wavelet (Fig. 3). We used shifted grids with the 12-th accuracy in space and the 2-nd accuracy in time.

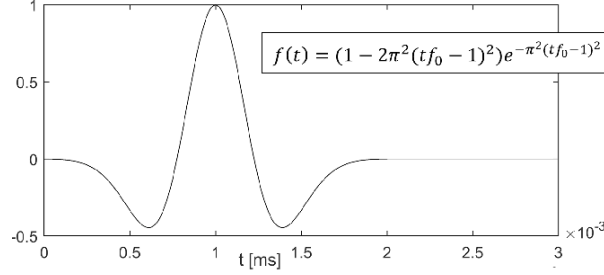


Figure 3: Ricker impulse, $f_0 = 40\text{Hz}$ - dominant frequency

The steps in space (0.005 km) and time (0.0004 s) satisfy the Courant condition $\Delta t < \Delta h / (kc_{\max}\sqrt{2})$, where parameter k depends on the order of approximation, in our case $k = 1, 34$. The calculation domain is rectangle $3.5\text{ km} \times 1\text{ km}$, the number of boundary points is $N_s = 151$. The sources are uniformly located on segment $[1.5\text{ km}, 2.5\text{ km}]$. Time T is 0.416 s .

After solving the forward problem, we tested the formula (7). Fig. 4 is the image computed for one source (no summation over α) and Fig. 5 is the image with summation over all sources.

To get such an image one need to have waves, which unknown in the inverse problem. Nevertheless, one can find waves v in the semi-geodesic coordinates in (9). Finding such waves leads to the problem of triangular factorization of the matrix C .

5 Triangular factorization and imaging

Our screen after discretization is a set of $N_s \times N_t$ points, N_s is the number of sources, and N_t is the number of time samples (in our case $N_s = 151$, $N_t = 150$). We parametrize points of the screen by greek letters, so that any $\sigma = 0, \dots, N_s \times N_t$ corresponds point (x_σ, τ_σ) of the screen. We arrange the points of the screen starting from the bottom left corner and ending with the top right one. We also associate any screen point α with a control, determined by source x_α and radius t_α of filling domain $B(x_\alpha, t_\alpha)$.

We replace integral

$$C_{\alpha\beta} = \int_{\Sigma} v(x', \tau, t_\alpha, x_\alpha) v(x', \tau, t_\beta, x_\beta) dx' d\tau$$

with sum

$$C_{\alpha\beta} = \sum_{\sigma=1}^{N_s \times N_t} v(x_\sigma, \tau_\sigma, t_\alpha, x_\alpha) v(x_\sigma, \tau_\sigma, t_\beta, x_\beta)$$

or in the matrix form

$$C = V^* V, \quad V_{\sigma\alpha} = v(x_\sigma, \tau_\sigma, t_\alpha, x_\alpha).$$

Due to kinematic reason matrix V is upper triangular. Indeed, let $\sigma > \alpha$. Then $\tau_\sigma \geq t_\alpha$. If $x_\sigma \neq x_\alpha$ then $\operatorname{dist}(\gamma(x_\sigma, \tau_\sigma), (x_\alpha, 0)) > \tau_\sigma \geq t_\alpha$ since τ_σ is the distance of point $\gamma(x_\sigma, \tau_\sigma)$ to the boundary. Therefore, $\gamma(x_\sigma, \tau_\sigma) \notin B(x_\alpha, t_\alpha)$. If $x_\sigma = x_\alpha$ then $\sigma > \alpha$ implies $\tau_\sigma > t_\alpha$ and again $\gamma(x_\sigma, \tau_\sigma) \notin B(x_\alpha, t_\alpha)$. In any case $\sigma > \alpha$ implies $u_t(\gamma(x_\sigma, \tau_\sigma), t_\alpha; x_\alpha) = 0$ and therefore $V_{\sigma\alpha} = 0$.

That is, to get waves on the screen, it suffices to perform a triangular factorization of the matrix C . The complexity of this problem is that C is ill-conditioned (but it is non-negative). We applied the following procedure for triangular factorization.

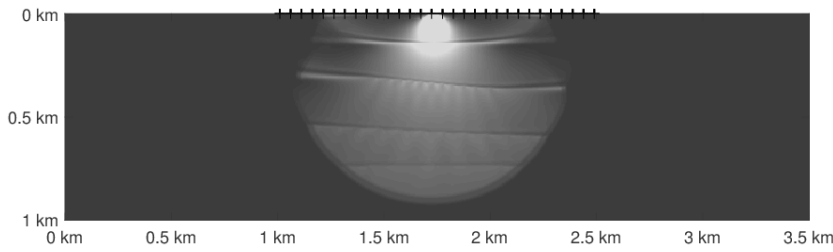


Figure 4: Image from one source

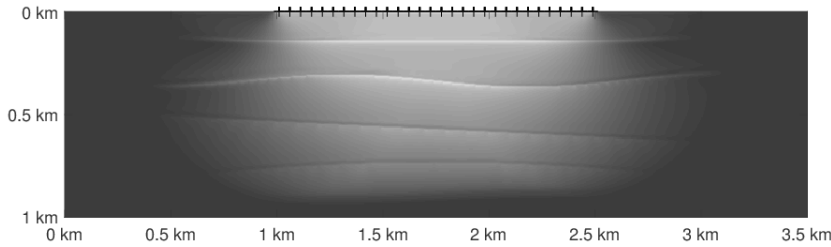


Figure 5: Image obtained after summation over all sources

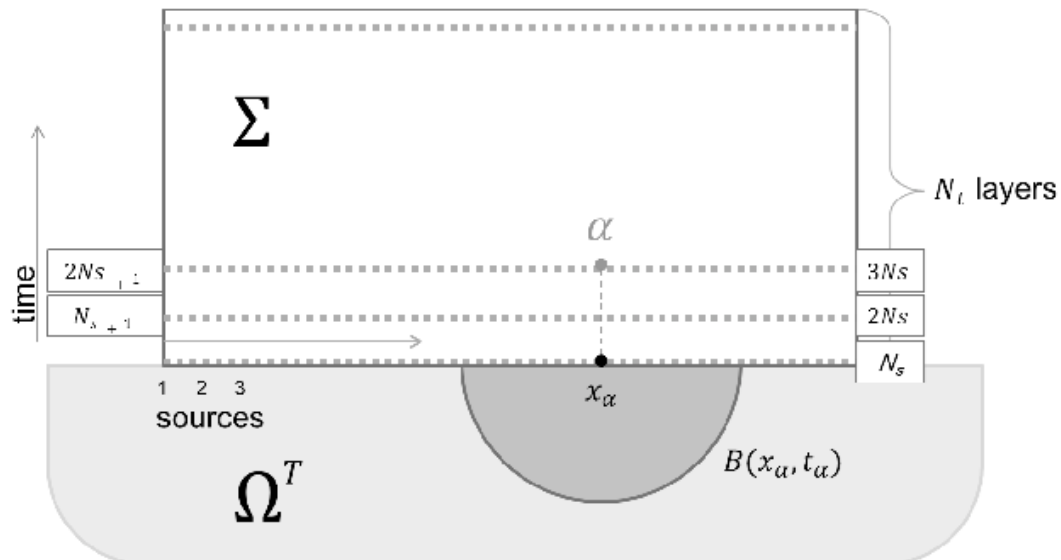
Assume that C is positive and let $C = X\Lambda X^*$ be its spectral decomposition, where matrix X is orthogonal and Λ is diagonal. Consider the QR decomposition of matrix $\sqrt{\Lambda}X^* = QR$, where Q is orthogonal and R is upper triangular. Then $C = X\sqrt{\Lambda}\sqrt{\Lambda}X^* = (QR)^*QR = R^*R$ and therefore $R = V$.

In our numerical experiment C had a few negative eigenvalues of small absolute value. We replaced Λ with $\Lambda + \alpha I$ with small positive α (we take α equals modulo of minimal eigenvalue): $\sqrt{\Lambda + \alpha I}X^* = Q_\alpha R_\alpha$ and obtain matrix R_α which we identify with V . Finally, we obtain the image in the semi-geodesic coordinates by the formula $F' = \text{diag}(R_\alpha R_\alpha^*)$ or

$$F'(x_\sigma, \tau_\sigma) = \sum_{\alpha=1}^{N_s \times N_t} v^2(x_\sigma, \tau_\sigma, t_\alpha, x_\alpha),$$

that corresponds to (10).

The resulting image (Fig. 7) contains some noise. Using a high-pass filter, we removed low frequencies for all columns of the image. (Each column corresponds to a normal ray intersecting inner

Figure 6: Screen Σ

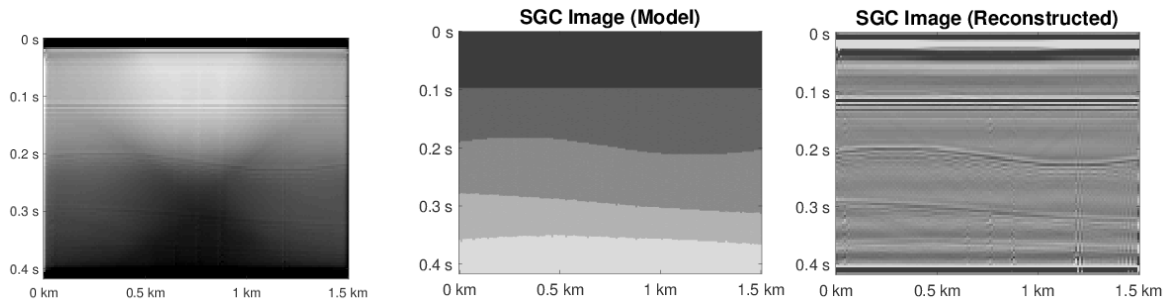


Figure 7: Reconstructed image in semi-geodetic coordinates

Figure 8: Model and reconstructed image after filtering in semi-geodetic coordinates

boundaries). This suppresses slow changes in image brightness, and we get an image in which the boundaries are enhanced. In the last two figures, we compare the image of our model, calculated in the semi-geodetic coordinates, and the reconstructed image after filtering.

If there is any approximation to the velocity, then it is easy to recalculate the image in the semi-geodetic coordinates into the corresponding Cartesian coordinates. Note that the image will retain the “correct” summation over the sources, regardless of this approximation. In the case of the reverse time or Kirchhoff migration, the incorrect velocity leads to out-of-phase summation of the waves.

Acknowledgments

The research was supported by a grant from the Russian Science Foundation (Project No. 23-21-00258, <https://www.rscf.ru/project/23-21-00258/>).

The authors would like to thank S.N. Sergeev for valuable help in filtering.

References

- [1] Zhu J., Lines L.R., *Comparison of Kirchhoff and reverse-time migration methods with applications to prestack depth imaging of complex structures*, Geophysics, 63.4 (1998), 1166-1176.
- [2] Sedaikina V.A., Pestov L.N., *Acoustical imaging in semi-geodesic coordinates without velocity knowledge*, Proceedings of the International Conference Days on Diffraction, DD 2016 (2016), 373-375.
- [3] Belishev M.I., Kachalov A.P., *An operator integral in the multidimensional spectral inverse problem*, Journal of Mathematical Sciences, 85.1 (1997), 1559-1564.
- [4] Belishev M.I., *TOPICAL REVIEW, Recent progress in the boundary control method*, Inverse Problems 23 (2007) R1-R67.
- [5] Belishev M.I., *Boundary control and tomography of Riemannian manifolds (BC-method)*, Russian Mathematical Surveys, 72.4 (2017), 581B-644.
- [6] Belishev M.I., Simonov S.A., *Triangular factorization and functional models of operators and systems*, Algebra and Analysis, 36 (2024), 1-28 (in Russian).
- [7] Belishev M., Gotlib Y.Y., *Dynamical variant of the BC-method: Theory and numerical testing*, J. Inverse Ill-Posed Probl., 7 (1999), 221-240.
- [8] Pestov L., Bolgova V., Kazarina O., *Numerical recovering of a density by the BC-method*, Inverse Probl. Imaging, 4 (2010), 703-712.
- [9] Belishev M.I., Ivanov I.B., Kubyshkin I.V., Semenov V.S., *Numerical testing in determination of sound speed from a part of boundary by the BC-method*, J. Inverse Ill-Posed Probl., 24 (2016), 159-180.
- [10] Ivanov I.B., Belishev M.I., Semenov V.S., *The Reconstruction of Sound Speed in the Marmousi Model by the Boundary Control Method*, preprint, <https://arxiv.org/abs/1609.07586>, 2016.
- [11] Oksanen L., *Solving an inverse obstacle problem for the wave equation by using the boundary control method*, Inverse Problems, 29 (2013), 035004.
- [12] Nosikova V.V., Pestov L.N., Sergeev S.N., Filatova V.M., *Reflected and scattered wave imaging by the Boundary Control Method, numerical experiment*, Zapiski Nauchnyh Seminarov POMI, 521 (2023), 200-211.

- [13] Ladyzhenskaya O.A., *The Boundary Value Problems of Mathematical Physics*, Applied Mathematical Sciences, vol. 49, Berlin; Heidelberg; New York: Springer Verlag, 1985.
- [14] Treves F., *Introduction to Pseudo-Differential and Fourier Integral Operators*, Plenum Press, New York and London, Vol. 1, 1982.
- [15] Belishev M.I., Blagovestchenskii A.S., *Multidimensional analogs of the Gel'fand-Levitan-Krein equations in inverse problem for the wave equation*, Ill-Posed Problems of Mathematical Physics and Analysis (Novosibirsk: Nauka), 1992, 50-63 (in Russian).

Vera Nosikova,
Immanuel Kant Baltic Federal University,
14 A. Nevskogo ul., Kaliningrad, 236016., Russia,
Email: vvnosikova@yandex.ru

Leonid Pestov,
Immanuel Kant Baltic Federal University,
14 A. Nevskogo ul., Kaliningrad, 236016., Russia,
Email: lpestov@kantiana.ru

Received 14.11.2024, Accepted 20.01.2025, Available online 30.09.2025.